



Synthesis and evaluation of coumarin/piperazine hybrids as acetylcholinesterase inhibitors

Juan Zhang^{1,2} · Cheng-Shi Jiang¹

Received: 22 March 2018 / Accepted: 23 April 2018
© Springer Science+Business Media, LLC, part of Springer Nature 2018

Abstract

A series of new coumarin/piperazine hybrids were synthesized and evaluated for anticholinesterase activity. Among them, compounds **4d** and **4t** exhibited potent human acetylcholinesterase (hAChE) inhibitory activity with IC_{50} values of 2.42 and 9.89 μ M, respectively, and **4t** displayed highest selectivity toward hAChE over human butyrylcholinesterase (hBChE) by 9.8-fold. In addition, both compounds did not show observed cytotoxicity against SH-SY5Y neuroblastoma cell line at 100 μ M. Kinetic analysis in tandem with molecular docking study revealed that these hybrids targeted both catalytic active site (CAS) and peripheral anionic site (PAS) of hAChE. The preliminary results highlighted **4t** as an anti-Alzheimer's disease lead compound worthy of further investigation.

Keywords Coumarin/piperazine hybrid · Acetylcholinesterase inhibitor · Molecular docking · Cytotoxicity · Alzheimer's disease

Introduction

Alzheimer's disease (AD) is an age-related neurodegenerative disorder, which was characterized by progressive memory loss, decline in language skills and cognitive functions. Now, AD has already become the third leading cause of death behind cancer and cardiovascular diseases. Currently, about 46.8 million people worldwide are suffering from AD, and this number will triple by 2050 with the aging of the population (Yu et al. 2017).

Although AD pathogenesis is very complex and still not fully understood, the low level of neurotransmitter acetylcholine (ACh) in brain was mainly related to cognitive and memory impairments of AD patients according to the cholinergic hypothesis of AD (Bartus et al. 1982). ACh can

be hydrolyzed by two types of cholinesterases, namely acetylcholinesterase (AChE) and butyrylcholinesterase (BChE). AChE is 10^{13} -fold more active than BChE, and almost accounts for nearly 80% ACh hydrolysis in brain (Feng et al. 2017). In this context, four out of five drugs approved by the FDA for anti-AD therapy are AChE inhibitors, i.e. donepezil, rivastigmine, galantamine, and tacrine as shown in Fig. 1 (Herrmann et al. 2011). However, tacrine was quickly withdrawn from the market due to its hepatotoxicity (Barreiro et al. 2003). Although the others could increase the concentration of ACh in brain to improve cognitive impairment, none of them can cure or stop the progress of AD (Weinstock 2012).

Compared with other AChE inhibitors on the market, donepezil still gets a great of attention due to its noticeable advantages, such as high bioavailability, few dose-limiting hepatotoxicity, long half-life, and relative fewer side effects (van Greunen et al. 2017). Therefore, lots of structural optimizations and structure-activity relationship (SAR) studies have been conducted on donepezil in order to develop more safe and effective AChE inhibitors. From the literature most inhibitors maintained the *N*-benzyl-piperidine of donepezil as this fragment could form important non-covalent bonds with key amino acid residues in the active site of AChE (Więckowska et al. 2015; Girisha et al. 2009). To mimic the piperidine ring in donepezil, piperazine scaffold as a bioisostere of piperidine have been extensively

Electronic supplementary material The online version of this article (<https://doi.org/10.1007/s00044-018-2185-x>) contains supplementary material, which is available to authorized users.

✉ Cheng-Shi Jiang
jiangchengshi-20@163.com

¹ School of Biological Science and Technology, University of Jinan, Jinan 250022, China

² Faculty of Ceilandia, University of Brasília, Brasília 72220275, Brazil

Fig. 1 Current and former AChE inhibitors approved for AD treatment

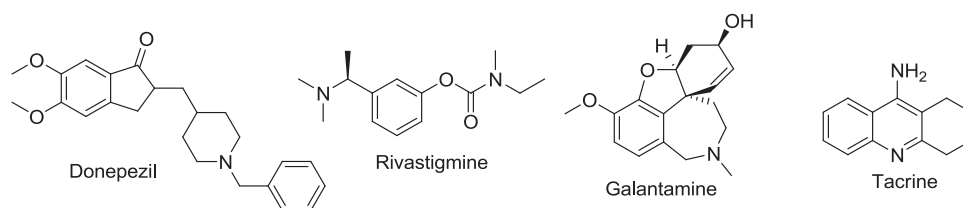
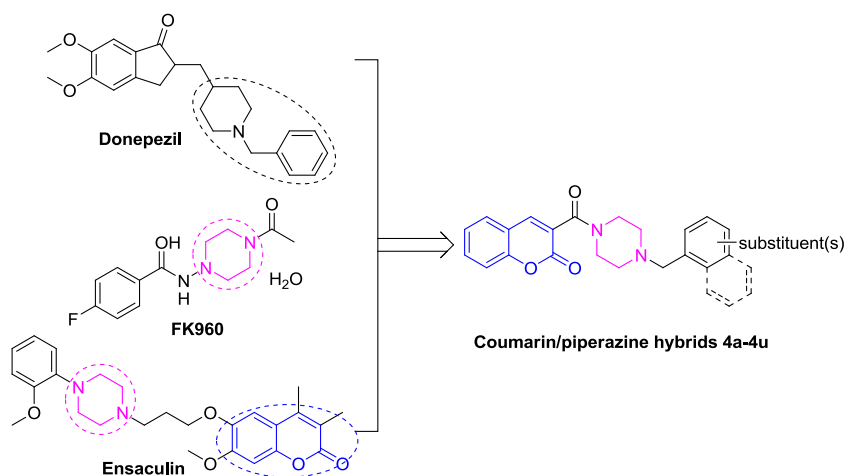


Fig. 2 Design of new coumarin/piperazine hybrids



exploited and various piperazine-based AChE inhibitors were developed (Demir Özkay et al. 2017). For example, a piperazine derivative FK960 exerted beneficial effects on memory deficits in AD rats and monkey (Matsuoka and Aigner 1997; Inoue et al. 2001). In addition, ensaculin (Fig. 2), a piperazine/coumarin conjugate, had been used in clinic as its HCl salt for treating AD for a long time (Hoerr and Noeldner 2002). It was worth mentioning that coumarin derivatives were usually found to have a broad-spectrum of biological activities, such as anti-viral (Hassan et al. 2016), anti-cancer (Dandriyal et al. 2016), anti-diabetic (Li et al. 2017), anti-inflammatory (Revankar et al. 2017), anti-microbial (Bhat et al. 2013), and anti-neurodegenerative activities (Jameel et al. 2016). In our project for seeking new anti-AD drug candidates, hybridization of coumarin and piperazine generated 21 derivatives as new candidates against AD. Herein, in the present study we describe the synthesis, biological evaluation and SAR study of this new series of coumarin/piperazine hybrid AChE inhibitors. In addition, the kinetic analysis and molecular docking were performed, and the cytotoxicity against SH-SY5Y cell of selected compounds were tested as well.

Materials and methods

Chemistry

Melting points were measured by a Melting Point YRY-3 apparatus (Tianjin Precision Apparatus Factory, China).

Commercially available reagents were used without further purification. Organic solvents were evaporated with reduced pressure using a Büchi R-100 evaporator. Reactions were monitored by thin layer chromatography (TLC) using GF254 silica gel plates (Yantai JingYou Silica Gel Inc., China). Silica gel column chromatography was performed on Biotage Isolera One and silica gel (200–300 mesh) from Qingdao Hailang Inc. (China). Purity data were recorded on an Agilent 1260 HPLC using parameters as follows: H₂O/MeOH, 40/60 to 0/100 in 15 min, 0/100 in 5 min, +5 min isocratic, flow rate of 1.0 mL/min, $\lambda = 280$ nm. NMR spectra were measured on Bruker Avance III 600 MHz spectrometers. Chemical shifts were expressed in δ (ppm) and coupling constants (J) in Hz with solvent signals as internal standards (CDCl₃, δ_{H} 7.26 ppm and δ_{C} 77.2 ppm; CD₃OD, δ_{H} 3.31 ppm and δ_{C} 49.0 ppm). ESI-MS analyses were performed on an Agilent 1260–6460 Triple Quad LC-MS instrument, and the elemental analysis was recorded on a Vario EL III (Elementar, Germany).

Synthesis of 2-oxo-2H-chromene-3-carboxylic acid (2)

In a round-bottomed flask 2-hydroxybenzaldehyde (2.44 g, 20 mmol) and Meldrum's acid (3.46 g, 24 mmol) in water (30 mL) were heated at reflux under stirring for 10 h. Then the reaction mixture was cooled and filtered on Büchner funnel. The products were purified by recrystallization from methanol to yield compound **2** as a white solid (3.61 g, 95% yield). m.p. 145–146 °C. ¹H NMR (600 MHz, MeOD) δ 8.82 (s, 1H), 7.83 (dd, $J = 8.1, 1.5$ Hz, 1H), 7.76 (ddd, $J =$

8.8, 7.5, 1.6 Hz, 1H), 7.45–7.41 (m, 2H). ^{13}C NMR (150 MHz, MeOD) δ 165.5, 160.8, 156.3, 151.1, 136.0, 131.4, 126.4, 119.7, 118.3, 117.6. ESI-MS m/z : 191.1 $[\text{M}+\text{H}]^+$.

4-(2-oxo-2H-chromene-3-carbonyl)piperazine-1-carboxylate (3)

To a solution of coumarin-3-carboxyl acid derivatives **2** (1.80 g, 9.5 mmol) in 30 mL dry dichloromethane (DCM) was added EDCI (2.18 g, 11.4 mmol), HOBT (1.28 mg, 9.5 mmol) and *N,N*-diisopropylethylamine (2.45 g, 19 mmol) at 0 °C. After 0.5 h, 1-Boc-piperazine (1.77 g, 9.5 mmol) was added, and the reaction mixture was stirred at room temperature for 16 h. The mixtures were concentrated and the residue was extracted by ethyl acetate (EtOAc) and water. The organic layers was combined, dried over MgSO_4 , and evaporated under reduced pressure. The residue was further purified by flash column chromatography with petroleum ether/EtOAc (1:1) to produced compound **3** as a white solid (2.87 g, 85% yield). m.p. 153–154 °C. ^1H NMR (600 MHz, CDCl_3) δ 7.95 (s, 1H), 7.61 (ddd, $J = 8.6, 7.4, 1.4$ Hz, 1H), 7.55 (dd, $J = 7.7, 1.2$ Hz, 1H), 7.37 (d, $J = 8.3$ Hz, 1H), 7.33 (dd, $J = 7.6, 7.4$ Hz, 1H), 3.74 (s, 2H), 3.55 (t, $J = 4.5$ Hz, 2H), 3.50 (t, $J = 4.5$ Hz, 2H), 3.36 (s, 2H), 1.47 (s, 9H). ^{13}C NMR (150 MHz, CDCl_3) δ 163.8, 158.1, 154.6, 154.3, 143.8, 133.2, 128.8, 125.1, 125.0, 118.0, 117.0, 80.5, 47.2, 42.3, 28.5. ESI-MS m/z : 359.1 $[\text{M}+\text{H}]^+$.

General procedure for synthesis of 4a–4u

To a stirred solution of **3** (100 mg, 0.28 mmol) in 5 mL DCM was added excessive amount of $\text{CF}_3\text{CO}_2\text{H}$ dropwise under nitrogen at 0 °C, and the reaction was monitored by TLC. The solvent was removed under reduced pressure to yield de-protection product as light yellow oil, which was used in next step without further purification.

Corresponding bromide (1 equiv) was added to a solution of above obtained oil and triethylamine (150 μL) in acetonitrile (5 mL) and the reaction mixture was stirred under reflux for 8 h. Subsequently, the solvent was evaporated under reduced pressure to get residue, which was purified by silica gel column chromatography to afford the desired products **4a–4u**, respectively.

3-(4-Benzylpiperazine-1-carbonyl)-2H-chromen-2-one (4a)

A white solid, yield 82%, m.p. 127–128 °C, HPLC purity: 97.20%, $t_{\text{R}} = 12.049$ min. ^1H NMR (600 MHz, CDCl_3) δ 7.90 (s, 1H), 7.58 (ddd, $J = 8.3, 7.4, 1.4$ Hz, 1H), 7.53 (dd, $J = 7.7, 1.4$ Hz, 1H), 7.35 (d, $J = 8.3$ Hz, 1H), 7.32 (m, 5H), 7.27 (m, 1H), 3.79 (brs, 2H), 3.55 (s, 2H), 3.40 (t, $J =$

5.0 Hz, 2H), 2.55 (t, $J = 5.0$ Hz, 2H), 2.48 (brs, 2H). ^{13}C NMR (150 MHz, CDCl_3) δ 163.5, 158.1, 154.2, 143.2, 137.7, 132.9, 129.3, 128.7, 128.5, 127.4, 125.4, 125.0, 118.4, 117.0, 62.9, 53.1, 52.6, 47.4, 42.3. ESI-MS m/z : 349.2 $[\text{M}+\text{H}]^+$. Anal: Calcd. for $\text{C}_{21}\text{H}_{20}\text{N}_2\text{O}_3$: C 72.40, H 5.79, N 8.04; found: C 72.33, H 5.68, N 8.16.

3-(4-(4-Methylbenzyl)piperazine-1-carbonyl)-2H-chromen-2-one (4b)

A light yellow solid, yield 77%, m.p. 125–126 °C, HPLC purity: 98.54%, $t_{\text{R}} = 13.376$ min. ^1H NMR (600 MHz, CDCl_3) δ 7.90 (s, 1H), 7.58 (ddd, $J = 8.3, 7.5, 1.4$ Hz, 1H), 7.53 (dd, $J = 7.7, 1.4$ Hz, 1H), 7.35 (d, $J = 8.3$ Hz, 1H), 7.32 (dd, $J = 7.7, 7.5$ Hz, 1H), 7.20 (d, $J = 7.9$ Hz, 2H), 7.13 (d, $J = 7.8$ Hz, 2H), 3.78 (t, $J = 5.0$ Hz, 2H), 3.51 (s, 2H), 3.43–3.34 (t, $J = 5.0$ Hz, 2H), 2.53 (t, $J = 5.0$ Hz, 2H), 2.47 (brs, 2H), 2.33 (s, 3H). ^{13}C NMR (150 MHz, CDCl_3) δ 163.5, 158.1, 154.2, 143.1, 137.1, 134.6, 132.9, 129.3, 129.2, 128.6, 125.4, 125.0, 118.4, 117.0, 62.6, 53.1, 52.5, 47.4, 42.3, 21.2. ESI-MS m/z : 363.2 $[\text{M}+\text{H}]^+$. Anal: Calcd. for $\text{C}_{22}\text{H}_{22}\text{N}_2\text{O}_3$: C 72.91, H 6.12, N 7.73; found: C 72.93, H 6.10, N 7.71.

3-(4-(3,5-Dimethylbenzyl)piperazine-1-carbonyl)-2H-chromen-2-one (4c)

A white solid, yield 89%, m.p. 219–220 °C, HPLC purity: 95.59%, $t_{\text{R}} = 14.569$ min. ^1H NMR (600 MHz, CDCl_3) δ 7.90 (s, 1H), 7.58 (ddd, $J = 8.5, 7.4, 1.1$ Hz, 1H), 7.53 (dd, $J = 7.6, 1.1$ Hz, 1H), 7.36 (d, $J = 8.5$ Hz, 1H), 7.32 (dd, $J = 7.6, 7.4$ Hz, 1H), 6.92 (s, 2H), 6.90 (s, 1H), 3.79 (brs, 2H), 3.47 (s, 2H), 3.40 (t, $J = 5.0$ Hz, 2H), 2.54 (t, $J = 5.0$ Hz, 2H), 2.47 (brs, 2H), 2.30 (s, 6H). ^{13}C NMR (150 MHz, CDCl_3) δ 163.4, 158.1, 154.2, 143.1, 138.0, 137.5, 132.9, 129.0, 128.6, 127.2, 125.5, 125.0, 118.5, 117.0, 63.0, 53.2, 52.7, 47.4, 42.3, 21.4. ESI-MS m/z : 377.1 $[\text{M}+\text{H}]^+$. Anal: Calcd. for $\text{C}_{23}\text{H}_{24}\text{N}_2\text{O}_3$: C 73.38, H 6.43, N 7.44; found: C 73.36, H 6.46, N 7.41.

3-(4-(3,5-Bis(trifluoromethyl)benzyl)piperazine-1-carbonyl)-2H-chromen-2-one (4d)

A light yellow solid, yield 92%, m.p. 170–171 °C, HPLC purity: 98.88%, $t_{\text{R}} = 14.883$ min. ^1H NMR (600 MHz, CDCl_3) δ 7.93 (s, 1H), 7.81 (s, 2H), 7.78 (s, 1H), 7.59 (ddd, $J = 8.5, 7.4, 1.4$ Hz, 1H), 7.54 (dd, $J = 7.6, 1.4$ Hz, 1H), 7.36 (d, $J = 8.5$ Hz, 1H), 7.33 (dd, $J = 7.6, 7.4$ Hz, 1H), 3.82 (brs, 2H), 3.65 (s, 2H), 3.42 (t, $J = 4.7$ Hz, 2H), 2.58 (t, $J = 5.0$ Hz, 2H), 2.51 (t, $J = 4.7$ Hz, 2H). ^{13}C NMR (150 MHz, CDCl_3) δ 163.6, 158.1, 154.3, 143.5, 140.9, 133.1, 131.8 (q, $J = 33.2$ Hz), 128.9, 128.70, 125.2, 125.1, 123.4 (q, $J = 129.1$ Hz), 121.5 (m), 118.41, 116.97, 61.77,

53.06, 52.70, 47.28, 42.20. ESI-MS m/z : 485.2 $[M+H]^+$. Anal: Calcd. for $C_{23}H_{18}F_6N_2O_3$: C 57.03, H 3.75, N 5.78; found: C 57.29, H 3.72, N 5.81.

3-(4-(4-Fluoro-2-methylbenzyl)piperazine-1-carbonyl)-2H-chromen-2-one (4e)

A light yellow solid, yield 85%, m.p. 120–121 °C, HPLC purity: 97.58%, t_R = 13.709 min. 1H NMR (600 MHz, $CDCl_3$) δ 7.90 (s, 1H), 7.58 (ddd, J = 8.6, 7.4, 1.5 Hz, 1H), 7.53 (dd, J = 7.6, 1.3 Hz, 1H), 7.35 (d, J = 8.3 Hz, 1H), 7.32 (dd, J = 7.6, 7.4 Hz, 1H), 7.17 (dd, J = 7.9, 6.4 Hz, 1H), 6.86 (dd, J = 9.7, 2.5 Hz, 1H), 6.81 (ddd, J = 8.4, 8.3, 2.6 Hz, 1H), 3.76 (brs, 2H), 3.46 (s, 2H), 3.37 (t, J = 4.2 Hz, 2H), 2.53 (brs, 2H), 2.46 (brs, 2H), 2.35 (s, 3H). ^{13}C NMR (150 MHz, $CDCl_3$) δ 163.5, 162.9, 161.3, 158.1, 154.2, 143.2, 140.1 (d, J = 7.8 Hz), 133.0, 131.50 (d, J = 8.0 Hz), 128.7, 125.3, 125.0, 118.4, 117.2 (d, J = 21.0 Hz), 116.9, 112.2 (d, J = 20.7 Hz), 60.1, 53.0, 52.5, 47.4, 42.3, 19.45 (d, J = 1.1 Hz). ESI-MS m/z : 381.2 $[M+H]^+$. Anal: Calcd. for $C_{22}H_{21}FN_2O_3$: C 69.46, H 5.56, N 7.36; found: C 69.49, H 5.57, N 7.34.

3-(4-(2,4-Difluorobenzyl)piperazine-1-carbonyl)-2H-chromen-2-one (4f)

A light yellow solid, yield 81%, m.p. 101–102 °C, HPLC purity: 98.80%, t_R = 12.247 min. 1H NMR (600 MHz, $CDCl_3$) δ 7.92 (s, 1H), 7.60 (ddd, J = 8.3, 7.5, 1.5 Hz, 1H), 7.54 (dd, J = 7.7, 1.4 Hz, 1H), 7.37–7.31 (m, 3H), 6.86 (ddd, J = 8.3, 8.1, 1.7 Hz, 1H), 6.81 (ddd, J = 8.4, 8.3, 1.4 Hz, 1H), 3.82 (brs, 2H), 3.66 (brs, 2H), 3.43 (s, 2H), 2.64 (brs, 4H). ^{13}C NMR (150 MHz, $CDCl_3$) δ 163.5, 162.4 (d, J = 12.1 Hz), 160.7 (d, J = 12.2 Hz), 158.2, 154.3, 143.5, 133.1, 132.7, 128.7, 125.1, 118.4, 117.0 (d, J = 21.0 Hz), 111.5 (d, J = 22.5 Hz), 104.0 (dd, J = 25.7, 25.9 Hz), 54.5, 52.6, 52.1, 47.0, 41.9. ESI-MS m/z : 385.2 $[M+H]^+$. Anal: Calcd. for $C_{21}H_{18}F_2N_2O_3$: C 65.62, H 4.72, N 7.29; found: C 65.65, H 4.70, N 7.26.

3-(4-(2,6-Difluorobenzyl)piperazine-1-carbonyl)-2H-chromen-2-one (4g)

A white solid, yield 88%, m.p. 145–146 °C, HPLC purity: 98.51%, t_R = 11.876 min. 1H NMR (600 MHz, $CDCl_3$) δ 7.88 (s, 1H), 7.58 (ddd, J = 8.3, 7.3, 1.4 Hz, 1H), 7.52 (dd, J = 7.3, 1.4 Hz, 1H), 7.35 (d, J = 8.3 Hz, 1H), 7.31 (dd, J = 7.5, 7.3 Hz, 1H), 7.24 (dd, J = 8.0, 7.7 Hz, 1H), 6.89 (dd, J = 7.7, 7.6 Hz, 2H), 3.78 (t, J = 4.5 Hz, 2H), 3.74 (s), 3.39 (t, J = 4.6 Hz, 2H), 2.61 (t, J = 4.6 Hz, 2H), 2.54 (brs, 2H). ^{13}C NMR (150 MHz, $CDCl_3$) δ 163.4, 162.2 (dd, J = 248.4, 8.2 Hz), 161.33 (d, J = 8.3 Hz), 158.1, 154.2, 143.2, 133.0, 129.7 (dd, J = 10.4, 10.3 Hz), 128.7, 125.3, 125.0, 118.4,

117.0, 112.49 (t, J = 20.0, 20.0 Hz), 111.4 (dd, J = 21.7, 5.0 Hz), 52.3, 51.7, 48.7, 47.3, 42.2. ESI-MS m/z : 385.2 $[M+H]^+$. Anal: Calcd. for $C_{21}H_{18}F_2N_2O_3$: C 65.62, H 4.72, N 7.29; found: C 65.60, H 4.74, N 7.33.

3-(4-(4-Bromo-2-fluorobenzyl)piperazine-1-carbonyl)-2H-chromen-2-one (4h)

A light yellow solid, yield 79%, m.p. 181–182 °C, HPLC purity: 98.15%, t_R = 13.938 min. 1H NMR (600 MHz, $CDCl_3$) δ 7.91 (s, 1H), 7.59 (ddd, J = 8.3, 7.4, 1.5 Hz, 1H), 7.53 (dd, J = 7.7, 1.3 Hz, 1H), 7.36 (d, J = 8.3 Hz, 1H), 7.32 (dd, J = 7.7, 7.4 Hz, 1H), 7.26 (m, 2H), 7.22 (dd, J = 9.8, 8.7 Hz, 1H), 3.79 (brs, 2H), 3.57 (s, 2H), 3.39 (t, J = 4.7 Hz, 2H), 2.57 (brs, 2H), 2.50 (brs, 2H). ^{13}C NMR (150 MHz, $CDCl_3$) δ 163.5, 162.1, 160.4, 158.1, 154.3, 143.4, 133.0, 132.46 (d, J = 5.0 Hz), 128.7, 127.5 (d, J = 3.6 Hz), 125.3, 125.1, 119.3, 119.1, 118.4, 117.0, 54.8, 52.9, 52.3, 47.3, 42.2. ESI-MS m/z : 445.0, 447.0 $[M+H]^+$. Anal: Calcd. for $C_{21}H_{18}BrFN_2O_3$: C 56.64, H 4.07, N 6.29; found: C 56.62, H 4.10, N 6.25.

3-(4-(4-Bromo-3-fluorobenzyl)piperazine-1-carbonyl)-2H-chromen-2-one (4i)

A white solid, yield 85%, m.p. 208–209 °C, HPLC purity: 98.17%, t_R = 13.741 min. 1H NMR (600 MHz, $CDCl_3$) δ 7.91 (s, 1H), 7.59 (ddd, J = 8.3, 7.4, 1.4 Hz, 1H), 7.54 (dd, J = 7.7, 1.2 Hz, 1H), 7.48 (dd, J = 7.8, 7.4 Hz, 1H), 7.36 (d, J = 8.3 Hz, 1H), 7.32 (dd, J = 7.7, 7.4 Hz, 1H), 7.15 (dd, J = 9.4, 1.5 Hz, 1H), 6.99 (dd, J = 8.1, 1.2 Hz, 1H), 3.79 (brs, 2H), 3.50 (s, 2H), 3.40 (t, J = 4.7 Hz, 2H), 2.54 (t, J = 5.0 Hz, 2H), 2.48 (t, J = 4.4 Hz, 2H). ^{13}C NMR (150 MHz, $CDCl_3$) δ 163.5, 160.0, 158.5, 158.1, 154.2, 143.4, 140.0, 133.4, 133.0, 125.7 (d, J = 3.3 Hz), 125.3, 125.1, 119.3, 118.4, 117.0, 116.9 (d, J = 22.4 Hz), 61.8, 53.0, 52.6, 47.4, 42.2. ESI-MS m/z : 445.1, 447.0 $[M+H]^+$. Anal: Calcd. for $C_{21}H_{18}BrFN_2O_3$: C 56.64, H 4.07, N 6.29; found: C 56.65, H 4.05, N 6.27.

3-(4-(2-(Trifluoromethyl)benzyl)piperazine-1-carbonyl)-2H-chromen-2-one (4j)

A white solid, yield 91%, m.p. 80–81 °C, HPLC purity: 97.09%, t_R = 14.035 min. 1H NMR (600 MHz, $CDCl_3$) δ 7.92 (s, 1H), 7.77 (d, J = 7.8 Hz, 1H), 7.63 (d, J = 7.8 Hz, 1H), 7.59 (ddd, J = 8.6, 7.0, 1.4 Hz, 1H), 7.54 (dd, J = 7.6, 1.3 Hz, 1H), 7.52 (d, J = 7.6 Hz, 1H), 7.36 (d, J = 8.6 Hz, 2H), 7.32 (dd, J = 7.6, 7.0 Hz, 1H), 3.81 (brs, 2H), 3.71 (s, 2H), 3.42 (t, J = 4.8 Hz, 2H), 2.58 (t, J = 4.8 Hz, 2H), 2.51 (brs, 2H). ^{13}C NMR (150 MHz, $CDCl_3$) δ 163.6, 158.1, 154.3, 143.3, 137.2, 133.0, 132.0, 130.4, 129.9, 128.90 (d, J = 30.2 Hz), 128.7, 127.2, 126.0 (q, J = 5.7 Hz, 2H),

125.4, 125.1, 118.4, 117.0, 58.2, 53.2, 52.7, 47.4, 42.4. ESI-MS m/z : 417.2 $[M+H]^+$. Anal: Calcd. for $C_{22}H_{19}F_3N_2O_3$: C 63.46, H 4.60, N 6.73; found: C 63.42, H 4.58, N 6.77.

3-(4-(4-(Trifluoromethyl)benzyl)piperazine-1-carbonyl)-2H-chromen-2-one (4k)

A white solid, yield 74%, m.p. 220–221 °C, HPLC purity: 95.77%, $t_R = 13.473$ min. 1H NMR (600 MHz, $CDCl_3$) δ 7.91 (s, 1H), 7.60–7.56 (m, 3H), 7.54 (d, $J = 7.7$, 1.4 Hz, 1H), 7.45 (d, $J = 8.0$ Hz, 2H), 7.36 (d, $J = 8.3$ Hz, 1H), 7.32 (dd, $J = 7.7$, 7.5 Hz, 1H), 3.80 (brs, 2H), 3.60 (s, 2H), 3.40 (t, $J = 4.7$ Hz, 2H), 2.54 (t, $J = 5.0$ Hz, 2H), 2.49 (t, $J = 4.7$ Hz, 2H). ^{13}C NMR (150 MHz, $CDCl_3$) δ 163.5, 158.1, 154.2, 143.3, 142.1, 133.0, 129.7 (q, $J = 32.3$ Hz), 129.3, 128.7, 125.4 (q, $J = 3.6$ Hz), 125.3, 125.1, 124.2 (q, $J = 271.9$ Hz), 118.4, 117.0, 62.3, 53.1, 52.6, 47.4, 42.3. ESI-MS m/z : 417.2 $[M+H]^+$. Anal: Calcd. for $C_{22}H_{19}F_3N_2O_3$: C 63.46, H 4.60, N 6.73; found: C 63.44, H 4.63, N 6.70.

3-(4-(2-Bromo-4-methoxybenzyl)piperazine-1-carbonyl)-2H-chromen-2-one (4l)

A light yellow solid, yield 92%, m.p. 164–165 °C, HPLC purity: 99.54%, $t_R = 14.096$ min. 1H NMR (600 MHz, $CDCl_3$) δ 7.91 (s, 1H), 7.58 (ddd, $J = 8.7$, 7.5, 1.1 Hz, 1H), 7.53 (dd, $J = 7.7$, 1.1 Hz, 1H), 7.41 (d, $J = 8.7$ Hz, 1H), 7.34 (t, $J = 7.5$ Hz, 1H), 7.32 (dd, $J = 7.7$, 7.5 Hz, 1H), 7.04 (d, $J = 3.0$ Hz, 1H), 6.68 (dd, $J = 8.7$, 3.1 Hz, 1H), 3.80 (brs, 2H), 3.78 (s, 3H), 3.59 (s, 2H), 3.41 (t, $J = 4.6$ Hz, 2H), 2.62 (t, $J = 5.0$ Hz, 2H), 2.55 (brs, 2H). ^{13}C NMR (150 MHz, $CDCl_3$) δ 163.52, 159.05, 158.08, 154.20, 143.22, 138.09, 133.43, 132.95, 128.66, 125.29, 125.03, 118.40, 116.92, 116.30, 115.02, 114.36, 61.64, 55.58, 53.05, 52.53, 47.39, 42.32. ESI-MS m/z : 374.2 $[M+H]^+$. Anal: Calcd. for $C_{22}H_{21}BrN_2O_4$: C 57.78, H 4.63, N 6.13; found: C 57.83, H 4.60, N 6.17.

3-(4-(3-Bromobenzyl)piperazine-1-carbonyl)-2H-chromen-2-one (4m)

A yellow solid, yield 77%, m.p. 118–119 °C, HPLC purity: 95.85%, $t_R = 13.697$ min. 1H NMR (600 MHz, $CDCl_3$) δ 7.91 (s, 1H), 7.59 (ddd, $J = 8.6$, 7.4, 1.5 Hz, 1H), 7.54 (dd, $J = 7.6$, 1.5 Hz, 1H), 7.50 (s, 1H), 7.40 (d, $J = 8.3$ Hz, 1H), 7.36 (d, $J = 8.3$ Hz, 1H), 7.32 (dd, $J = 7.6$, 7.4 Hz, 1H), 7.24–7.21 (m, 1H), 7.20–7.18 (m, 1H), 3.80 (brs, 2H), 3.52 (s, 2H), 3.41 (brs, 2H), 2.56 (brs, 2H), 2.49 (brs, 2H). ^{13}C NMR (150 MHz, $CDCl_3$) δ 163.5, 158.2, 154.2, 143.3, 133.0, 132.1, 130.8, 130.2, 130.1, 128.7, 127.8, 125.4, 125.1, 122.7, 118.4, 117.0, 62.2, 53.0, 52.6, 47.3, 42.2.

ESI-MS m/z : 427.0 $[M+H]^+$. Anal: Calcd. for $C_{21}H_{19}BrN_2O_3$: C 59.03, H 4.48, N 6.56; found: C 59.09, H 4.50, N 6.60.

3-(4-(4-Bromobenzyl)piperazine-1-carbonyl)-2H-chromen-2-one (4n)

A white solid, yield 65%, m.p. 213–214 °C, HPLC purity: 97.16%, $t_R = 13.710$ min. 1H NMR (600 MHz, $CDCl_3$) δ 7.91 (s, 1H), 7.59 (ddd, $J = 8.3$, 7.4, 1.5 Hz, 1H), 7.53 (dd, $J = 7.6$, 1.3 Hz, 1H), 7.44 (d, $J = 8.3$ Hz, 2H), 7.36 (d, $J = 8.3$ Hz, 1H), 7.32 (t, $J = 7.6$, 7.4 Hz, 1H), 7.20 (d, $J = 8.2$ Hz, 2H), 3.76 (brs, 2H), 3.49 (s, 2H), 3.39 (t, $J = 4.6$ Hz, 2H), 2.53 (t, $J = 4.8$ Hz, 2H), 2.47 (brs, 2H). ^{13}C NMR (150 MHz, $CDCl_3$) δ 163.50, 158.13, 154.25, 143.29, 136.87, 133.00, 131.62, 130.85, 128.68, 125.35, 125.07, 121.26, 118.44, 116.98, 62.16, 53.05, 52.55, 47.37, 42.29. ESI-MS m/z : 427.1, 429.1 $[M+H]^+$. Anal: Calcd. for $C_{21}H_{19}BrN_2O_3$: C 59.03, H 4.48, N 6.56; found: C 58.98, H 4.44, N 6.51.

Methyl 4-((4-(2-oxo-2H-chromene-3-carbonyl)piperazin-1-yl)methyl)benzoate (4o)

A light yellow solid, yield 78%, m.p. 180–181 °C, HPLC purity: 95.38%, $t_R = 11.742$ min. 1H NMR (600 MHz, $CDCl_3$) δ 8.00 (d, $J = 8.2$ Hz, 2H), 7.91 (s, 1H), 7.59 (ddd, $J = 8.2$, 7.4, 1.4 Hz, 1H), 7.53 (dd, $J = 7.6$, 1.4 Hz, 1H), 7.42 (d, $J = 6.9$ Hz, 1H), 7.36 (d, $J = 8.3$ Hz, 1H), 7.32 (dd, $J = 7.6$, 7.4 Hz, 1H), 3.91 (s, 2H), 3.81 (brs, 2H), 3.61 (brs, 2H), 3.42 (brs, 2H), 2.57 (brs, 2H), 2.51 (brs, 2H). ^{13}C NMR (150 MHz, $CDCl_3$) δ 167.1, 165.6, 163.5, 158.2, 154.2, 143.4, 133.0, 129.9, 129.1, 128.7, 125.3, 125.1, 118.4, 117.0, 62.4, 53.1, 52.6, 52.3, 47.3, 42.2. ESI-MS m/z : 407.2 $[M+H]^+$. Anal: Calcd. for $C_{23}H_{22}N_2O_5$: C 67.97, H 5.46, N 6.89; found: C 67.94, H 5.50, N 6.94.

3-(4-(4-(Methylsulfonyl)benzyl)piperazine-1-carbonyl)-2H-chromen-2-one (4p)

A light yellow solid, yield 78%, m.p. 174–175 °C, HPLC purity: 95.62%, $t_R = 7.873$ min. 1H NMR (600 MHz, $CDCl_3$) δ 7.91–7.88 (m, 3H), 7.91 (s, 1H), 7.59 (ddd, $J = 8.5$, 7.4, 1.4 Hz, 1H), 7.56–7.53 (m, 13H), 7.35 (d, $J = 8.5$ Hz, 1H), 7.32 (dd, $J = 7.6$, 7.4 Hz, 1H), 3.79 (brs, 2H), 3.63 (s, 2H), 3.41 (brs, 2H), 3.05 (s, 3H), 2.56 (brs, 2H), 2.50 (brs, 2H). ^{13}C NMR (150 MHz, $CDCl_3$) δ 163.5, 158.1, 154.2, 147.5, 143.4, 139.6, 133.1, 129.8, 128.7, 127.6, 127.3, 125.1, 118.4, 116.9, 62.1, 53.1, 52.6, 52.3, 47.3, 44.6, 42.2. ESI-MS m/z : 427.1 $[M+H]^+$. Anal: Calcd. for $C_{22}H_{22}N_2O_5S$: C 61.96, H 5.20, N 5.20, S 7.52; found: C 67.94, H 5.50, N 6.94.

4-((4-(2-Oxo-2H-chromene-3-carbonyl)piperazin-1-yl)methyl)benzotrile (4q)

A light yellow solid, yield 87%. m.p. 210–211 °C, HPLC purity: 97.77%, $t_R = 10.200$ min. ^1H NMR (600 MHz, CDCl_3) δ 7.92 (s, 1H), 7.62 (d, $J = 8.2$ Hz, 2H), 7.59 (ddd, $J = 8.3, 7.4, 1.4$ Hz, 1H), 7.54 (dd, $J = 7.6, 1.4$ Hz, 1H), 7.46 (d, $J = 8.1$ Hz, 2H), 7.36 (d, $J = 8.3$ Hz, 1H), 7.33 (dd, $J = 7.6, 7.4$ Hz, 1H), 3.80 (brs, 2H), 3.59 (s, 2H), 3.40 (t, $J = 4.6$ Hz, 2H), 2.55 (t, $J = 5.0$ Hz, 2H), 2.49 (t, $J = 4.7$ Hz, 2H). ^{13}C NMR (150 MHz, CDCl_3) δ 163.5, 158.1, 154.3, 143.7, 143.4, 133.1, 132.4, 129.6, 128.7, 125.3, 125.1, 119.0, 118.4, 117.0, 111.3, 62.3, 53.1, 52.7, 47.3, 42.3. ESI-MS m/z : 374.2 $[\text{M}+\text{H}]^+$. Anal: Calcd. for $\text{C}_{22}\text{H}_{19}\text{N}_3\text{O}_3$: C 70.76, H 5.13, N 11.25; found: C 70.70, H 5.16, N 11.28.

Methyl (E)-3-(4-((4ethyl (E)-3-(4-((2-oxo-2H-chromene-3-carbonyl)piperazin-1-yl)methyl)phenyl)acrylate (4r)

A white solid, yield 78%, m.p. 212–213 °C, HPLC purity: 99.09%, $t_R = 12.760$ min. ^1H NMR (600 MHz, CDCl_3) δ 7.91 (s, 1H), 7.68 (d, $J = 16.0$, 1H), 7.59 (ddd, $J = 8.4, 7.6, 1.4$ Hz, 1H), 7.53 (dd, $J = 7.7, 1.1$ Hz, 1H), 7.48 (d, $J = 8.0$ Hz, 2H), 7.36–7.3 (m, 3H), 7.32 (dd, $J = 7.6, 7.4$ Hz, 1H), 6.43 (d, $J = 16.0$, 1H), 3.80 (s, 3H), 3.79 (brs, 2H), 3.56 (s, 2H), 3.40 (t, $J = 4.5$ Hz, 2H), 2.55 (t, $J = 4.8$ Hz, 2H), 2.49 (brs, 2H). ^{13}C NMR (150 MHz, CDCl_3) δ 167.6, 163.5, 158.1, 154.2, 144.7, 143.3, 140.5, 133.6, 133.0, 129.6, 128.7, 128.3, 125.4, 125.1, 118.4, 117.7, 117.0, 62.5, 53.1, 52.6, 51.9, 47.4, 42.3. ESI-MS m/z : 433.2 $[\text{M}+\text{H}]^+$. Anal: Calcd. for $\text{C}_{25}\text{H}_{24}\text{N}_2\text{O}_5$: C 69.43, H 5.59, N 4.68; found: C 69.49, H 5.56, N 4.66.

2-((4-(2-Oxo-2H-chromene-3-carbonyl)piperazin-1-yl)methyl)benzotrile (4s)

A yellow solid, yield 91%, m.p. 164–165 °C, HPLC purity: 99.56%, $t_R = 10.582$ min. ^1H NMR (600 MHz, CDCl_3) δ 7.97 (s, 1H), 7.70 (dd, $J = 7.8, 0.8$ Hz, 1H), 7.67–7.58 (m, 3H), 7.56 (dd, $J = 7.7, 1.4$ Hz, 1H), 7.46 (td, $J = 7.6, 1.1$ Hz, 1H), 7.38–7.31 (m, 2H), 4.04 (s, 2H), 3.92 (brs, 2H), 3.54 (t, $J = 4.6, 2\text{H}$), 2.91 (brs, 4H). ^{13}C NMR (150 MHz, CDCl_3) δ 163.5, 158.3, 154.3, 144.4, 133.4, 133.4, 133.3, 131.3, 129.3, 128.9, 125.2, 124.5, 118.3, 117.6, 117.0, 113.9, 59.4, 52.5, 51.9, 46.0, 41.0. ESI-MS m/z : 374.2 $[\text{M}+\text{H}]^+$. Anal: Calcd. for $\text{C}_{22}\text{H}_{19}\text{N}_3\text{O}_3$: C 70.76, H 5.13, N 11.25; found: C 70.80, H 5.09, N 11.30.

3-(4-(Naphthalen-1-ylmethyl)piperazine-1-carbonyl)-2H-chromen-2-one (4t)

A yellow solid, yield 77%, m.p. 118–119 °C, HPLC purity: 95.28%, $t_R = 14.574$ min. ^1H NMR (600 MHz, CDCl_3) δ

8.32–8.26 (m, 1H), 7.90 (s, 1H), 7.85 (dd, $J = 7.8, 1.5$ Hz, 1H), 7.79 (dd, $J = 6.8, 2.5$ Hz, 1H), 7.59 (ddd, $J = 8.4, 7.4, 1.5$ Hz, 1H), 7.55–7.48 (m, 3H), 7.42–7.38 (m, 2H), 7.35 (d, $J = 8.4$ Hz, 1H), 7.32 (dd, $J = 7.6, 7.4$ Hz, 1H), 3.95 (s, 2H), 3.78 (brs, 2H), 3.38 (t, $J = 4.7$ Hz, 2H), 2.63 (t, $J = 5.0$ Hz, 2H), 2.55 (brs, 2H). ^{13}C NMR (150 MHz, CDCl_3) δ 163.5, 158.1, 154.2, 143.1, 134.0, 133.5, 132.9, 132.6, 128.6, 128.7, 128.4, 127.8, 126.0, 125.9, 125.4, 125.2, 125.0, 124.8, 118.4, 117.0, 61.2, 53.2, 52.8, 47.4, 42.4. ESI-MS m/z : 427.0 $[\text{M}+\text{H}]^+$. Anal: Calcd. for $\text{C}_{25}\text{H}_{22}\text{N}_2\text{O}_3$: C 75.36, H 5.57, N 7.03; found: C 75.30, H 5.60, N 7.05.

3-(4-([1,1'-Biphenyl]-4-ylmethyl)piperazine-1-carbonyl)-2H-chromen-2-one (4u)

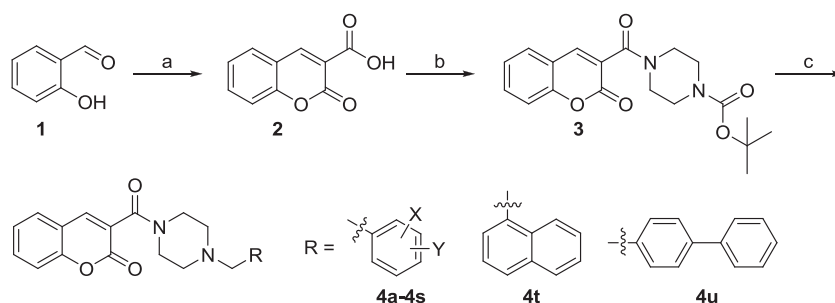
A white solid, yield 89%, m.p. 178–179 °C, HPLC purity: 98.54%, $t_R = 13.376$ min. ^1H NMR (600 MHz, CDCl_3) δ 7.91 (s, 1H), 7.59 (m, 3H), 7.56 (d, $J = 8.2$ Hz, 2H), 7.54 (dd, $J = 7.8, 1.5$ Hz, 1H), 7.44 (dd, $J = 8.0, 7.4$ Hz, 2H), 7.39 (d, $J = 8.2$ Hz, 2H), 7.35 (m, 3H), 3.81 (brs, 2H), 3.59 (s, 2H), 3.42 (t, $J = 4.8, 2\text{H}$), 2.59 (t, $J = 4.8, 2\text{H}$), 2.53 (brs, 2H). ^{13}C NMR (150 MHz, CDCl_3) δ 163.5, 158.1, 154.2, 143.2, 141.0, 140.4, 136.8, 133.0, 129.7, 128.9, 128.7, 127.4, 127.2, 127.2, 125.4, 125.0, 118.4, 117.0, 62.6, 53.2, 52.6, 47.4, 42.4. ESI-MS m/z : 425.1 $[\text{M}+\text{H}]^+$. Anal: Calcd. for $\text{C}_{27}\text{H}_{24}\text{N}_2\text{O}_3$: C 76.40, H 5.70, N 6.60; found: C 76.35, H 5.74, N 6.58.

Evaluation of hAChE and hBChE inhibitory activity

AChE and BChE inhibitory activities of all the target compounds were determined by using modified Ellman's method (Ellman et al. 1961; Talesa 2001). Human recombinant AChE, human plasmatic BChE, 5,5'-dithiobis(2-nitrobenzoic acid) (DTNB), phosphate buffer solution (PBS, pH 8.0), acetylthiocholine (ATC) iodide, and butyrylthiocholine (BUC) iodide were purchased from Sigma-Aldrich (Steinheim, Germany). Donepezil was used as positive control. Enzyme solutions were prepared at 2.0 U/mL in 2 mL aliquots. The assay medium consisted of 10 μL of enzyme, 40 μL of PBS, 20 μL of 0.01 M DTNB and 10 μL of tested compound. Assayed solutions of tested compounds were pre-incubated with corresponding ChE for 5 min. The reaction was initiated by addition of 20 μL of 0.01 M substrate (ATC or BUC). The activity was determined by measuring the increase in absorbance at 410 nm at 37 °C in 2 min intervals using Tecan Spark multimode microplate reader (Switzerland). The percentage of inhibition (I) was calculated from the measured data as follows: $I = (A_c - A_i)/A_c \times 100\%$, where A_i and A_c represent the change in the absorbance in the presence of inhibitor and without inhibitor, respectively.

Scheme 1 Synthesis of **4a–4u**.

Reaction conditions and reagents: **a** Meldrum's acid, H₂O, reflux, 10 h; **b** 1-Boc-piperazine, EDCI, HOBT, DCM, DIEPA, 16 h; **c** (1) CF₃CO₂H, DCM, 0 °C; (2) RCH₂Br, Et₃N, acetone, 80 °C for 8 h

**Kinetic assay**

Kinetic studies of inhibition on AChE were performed by using Ellman's method as described above. The concentrations of used substrates were 0.07813, 0.1563, 0.3125, and 0.625 μ M. Linear regression was used for calculation of Lineweaver-Burk plots, and all the calculations were performed using GraphPad Prism 5.0 software.

Molecular docking

Molecular docking were performed by using the Autodock 4.2 program (Morris et al. 1998; Huey et al. 2007). The crystal structure of the hAChE complexed with donepezil (PDB 4EY7) was obtained from the Protein Data Bank after removing the inhibitor and water molecules. The 3D Structure of **4t** was built by performing MM2 minimize energy in ChemBio3D Ultra 11.0. Using Autodock Tools 1.5.6, preparation of receptor was made by addition of hydrogen atoms and Gasteiger charges, and finally assignment of atomic types as AD4 type, and then autotorsions was used to define the rotatable bonds in the ligand preparation. The resulting enzyme structure was used as an input for the Autogrid program, which performed a pre-calculated atomic affinity grid maps for each atom type in the ligand plus an electrostatics map and a separate desolvation map presented in the substrate molecule. The dimensions of the box were set to 60 \times 60 \times 60 with grid spacing of 0.375 Å. Rigid ligand docking was performed for the compounds. Docking calculations were carried out using the Lamarckian genetic algorithm.

In vitro cytotoxicity evaluation

Cytotoxicity of selected compounds were evaluated against SH-SY5Y neuroblastoma cell line according to a reported protocol (Mosmann 1983), with donepezil as positive control. SH-SY5Y cell were inoculated into 96-well plates. After incubation for 24 h, the cells were treated with different concentrations of tested compounds for 24 h and then were incubated with 10 μ L of 3-(4,5-dimethylthiazol-2-yl)-2,5-diphenyltetrazolium bromide (MTT) at 37 °C for 2 h.

The formazan dye product was measured by the absorbance at 490 nm on a Tecan Spark multimode microplate reader (Switzerland).

Results and discussion**Chemical synthesis**

The synthesis of coumarin/piperazine hybrids **4a–4u** was shown in Scheme 1. Coumarin-3-carboxylic acid **2** was prepared from the reaction of Meldrum's acid with 2-hydroxybenzaldehyde. Then compound **3** was obtained by EDCI condensation in the presence of **2** and Boc-piperazine. Finally, the reaction between deprotection product of **3** and different bromides yielded the corresponding target compounds **4a–4u**. All the prepared compounds were confirmed by using ¹H NMR, ¹³C NMR, MS and elemental analysis data. All the spectra of compounds have been provided in supporting information.

AChE and BChE inhibition assay

The inhibitory activities of hybrids **4a–4u** against human recombinant AChE (hAChE) and human plasmatic BChE (hBChE) were evaluated with donepezil as reference compound. The results were summarized in Table 1. Nearly all the tested compounds showed inhibition on hAChE with IC₅₀ values ranging 2.42 to 80.78 μ M, except **4r** and **4u** (IC₅₀ values > 100 μ M). Compared with compound **4a**, the methyl substituent(s) in **4b** and **4c** did not show significant effect on the activity. Since the fluorinated functionalities were reported as key pharmacophore found in about 20% pharmaceutical on the market (Furuya et al. 2011), the F-substituted analogs **4d–4k** were then prepared. Among them, compound **4d** with 3,5-bistrifluoromethyl displayed the most potent activity (IC₅₀ = 2.42 μ M), while compound **4k** with 4-trifluoromethyl exhibited decreased activity (IC₅₀ = 62.87 μ M) and compounds **4o–4r** with electron-withdrawing groups (cyano, methyl carboxylate, methylsulfonyl, and methyl acrylate) at *para*-position showed weak activity. This result indicated that strong electron-withdrawing group at

Table 1 In vitro inhibition on hAChE and hBChE

Compounds	x,y	IC ₅₀ (μM) ± SD ^a		Selectivity for hAChE ^b
		hAChE	hBChE	
4a	H	32.28 ± 0.34	41.96 ± 0.22	1.3
4b	4-CH ₃	32.79 ± 0.06	20.51 ± 0.01	0.6
4c	3-CH ₃ , 5-CH ₃	30.75 ± 0.03	15.67 ± 0.12	0.5
4d	3-CF ₃ , 5-CF ₃	2.42 ± 0.15	3.87 ± 0.23	1.6
4e	2-CH ₃ , 4-F	27.04 ± 0.12	32.45 ± 0.78	1.2
4f	2-F, 4-F	15.54 ± 0.06	34.19 ± 0.01	2.2
4g	2-F, 6-F	20.78 ± 0.56	29.09 ± 0.33	1.4
4h	2-F, 4-Br	18.96 ± 0.31	9.48 ± 0.22	0.5
4i	3-F, 4-Br	42.04 ± 0.34	46.24 ± 0.85	1.1
4j	2-CF ₃	15.53 ± 0.24	27.22 ± 0.08	1.8
4k	4-CF ₃	62.87 ± 0.44	69.16 ± 0.19	1.1
4l	2-Br, 4-OCH ₃	18.66 ± 0.81	14.93 ± 0.04	0.8
4m	3-Br	12.03 ± 0.01	21.04 ± 0.33	1.7
4n	4-Br	42.04 ± 0.34	17.63 ± 0.67	2.4
4o	4-CO ₂ Me	55.28 ± 0.17	82.92 ± 1.33	1.5
4p	4-SO ₂ Me	57.78 ± 0.32	75.11 ± 0.89	1.3
4q	4-CN	80.78 ± 0.17	>100	–
4r	4,  CO ₂ Me	>100	>100	–
4s	2-CN	33.28 ± 0.66	16.64 ± 0.27	0.5
4t	–	8.78 ± 0.22	86.04 ± 0.76	9.8
4u	–	>100	>100	–
donepezil		0.03 ± 0.01	4.31 ± 0.76	144

^aIC₅₀ (hBChE)/IC₅₀ (hAChE)^bResults are expressed as the mean of 3 independent experiments

meta-position of benzene ring might be favorable for increased AChE inhibitory activity, and the electron-withdrawing group at *para*-position of benzene resulted in decreased inhibition on AChE. Next, the effect of aromatic property of substituent on bioactivity was investigated, the naphthalene group was first introduced to the piperazine based on the observation that naphthalene was capable of increasing the inhibitory activity and selectivity toward AChE in our previous study (Li et al. 2016). Interestingly, although compound **4t** with naphthalene group showed slightly weaker inhibition on AChE than **4d**, it had the highest selectivity toward AChE over BChE by 9.8-fold. However, the introduction of another aromatic system, biphenyl, made the activity loss (**4u**, IC₅₀ > 100 μM), probably due to its steric hindrance. Compared with the activity of donepezil, further structural modifications on this series of hybrids to improve their potency and selectivity are still need.

Kinetic assay

Since compound **4t** showed promising inhibitory activity and highest selectivity toward hAChE, it was selected as a representative compound of this series for kinetic assay to

obtain information about the inhibition mode and binding site. The mechanism of AChE inhibition was analyzed by recording substrate concentration-enzyme velocity curves in the presence of different concentration of **4t**.

As shown in Fig. 3a, it revealed both decreasing V_{max} and increasing K_{max} at rising concentrations of **4t** (Fig. 3). The equilibrium constants for binding with the free enzyme (K_I) and with the enzyme-substrate complex (K_{IS}) were obtained from the slope and the $1/V_{max}$ values plotted against inhibitor concentration, respectively (Delogu et al. 2016). The values of K_I (Fig. 3b) and K_{IS} (Fig. 3c) of **4t** were determined to be 3.29 and 11.47 μM for hAChE, respectively. These patterns indicated that compound **4t** was a linear-mixed type AChE inhibitor, suggesting that **4t** may not only compete with the substrate for the catalytic active site (CAS) but also interact with the second binding site, peripheral anionic site (PAS). This was in agreement with the subsequent result from molecular modeling study of **4t** (Fig. 4).

Molecular modeling study

The probable binding mode of compound **4t** with the catalytic domain of AChE (PDB: 4EY7) (Cheung et al. 2012)

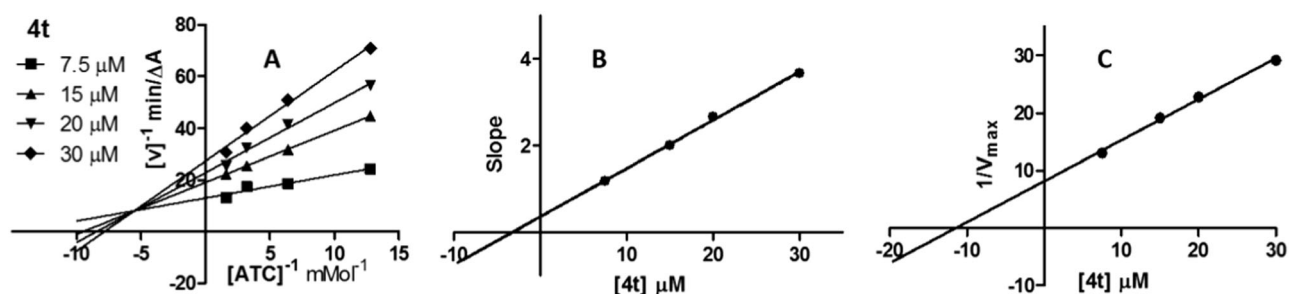


Fig. 3 Kinetic assay on AChE inhibition displayed by **4t**. **a** Lineweaver–Burk reciprocal plots of initial velocity and increasing substrate concentrations (0.078–0.625 mM); **b** Secondary plot of slopes versus **4t** concentrations; **c** Secondary plot of $1/V_{\max}$ versus **4t** concentrations

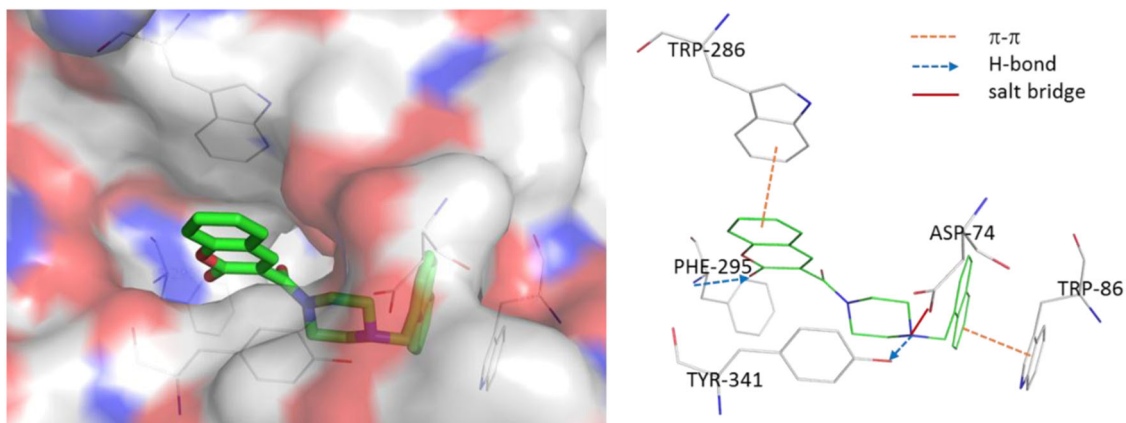


Fig. 4 The docking of **4t** (carbon in green) in the catalytic site of AChE with only the primary interactions shown

was investigated by molecular docking, which was performed by using Autodock 4.2 (Morris et al. 1998; Huey et al. 2007). The structure images was created by Pymol 1.5. As shown in Fig. 4, compound **4t** was bound very well to the active-gorge of AChE, with coumarin fragment oriented in the PAS and naphthalene moiety located in the CAS. There are three kinds of primary interactions between **4t** and the key amino acid residues in the active-site of AChE, including H-bond, π - π and salt bridge interactions. For example, the coumarin and naphthalene moieties could form π - π interactions with Trp286 and Trp86, respectively, and the carbonyl in coumarin interacts with Phe295 via forming H-bond. The protonated nitrogen atom in the piperazine ring could form H-bond interaction with Try341 and salt bridge with Asp74. In addition, the hydrophobic interactions between **4t** and the surrounding key amino acid residues (Try337, Trp286, Phe338, Try341, and Trp 86) also contribute to the affinity of ligand and AChE.

In addition, molecular docking was also performed for **4t**/BChE by using Autodock 4.2 to explain its selectivity toward AChE and BChE. The result of docking result of **4t**/BChE (Fig. S1, ESI⁺) indicated that **4t** could also be protonated in the active pocket of BChE (PDB: 4BDS) (Nachon et al. 2013) but it showed fewer interactions with the amino acid

residues in active site of BChE compared with the binding mode of **4t**/AChE. This was speculated to be a reason that **4t** exhibited good selectivity toward AChE over BChE.

In vitro cytotoxicity

The toxicity profile of active compound is usually considered throughout the process of drug research and development. Herein, the in vitro cytotoxicity of compounds **4d** and **4t**, which showed IC_{50} values less than 10 μ M in AChE assay, were selected to be evaluated against SH-SY5Y neuroblastoma cell line, using MTT assay with donepezil as reference compound. The results in Table 2 demonstrated that both hybrids did not exhibit observed cytotoxic effect on SH-SY5Y cell, with very low inhibition rate at 100 μ M, indicating that they are much less cytotoxic than donepezil ($IC_{50} = 20.8 \mu$ M).

Conclusion

In summary, 21 novel derivatives were prepared based on the hybridization of coumarin and piperazine pharmacophores, and were subjected to the in vitro hAChE and

Table 2 The cytotoxicity of compounds

Compound	SH-SY5Y 100 μM^{a}	IC ₅₀ (μM)
4d	5.4%	>100 ^b
4t	4.4%	>100
donepezil	89.1%	20.8

^aInhibition ratio at 100 μM

^bCompound with inhibition ratio less than 50% at 100 μM was not tested further

hBChE inhibition assay. Among the synthesized analogs, compounds **4d** and **4t** afforded IC₅₀ values ranging from 2.42 to 9.89 μM against hAChE with no observed cytotoxicity against SH-SY5Y cell at 100 μM . Especially, **4t** showed high selectivity toward hAChE over hBChE by 9.8-fold. The kinetic assay and molecular modeling study revealed these compounds as dual binding site AChE inhibitors. The present study demonstrated that these coumarin/piperazine hybrids serve as a new template for developing novel potent and safe AChE inhibitors.

Acknowledgements This research work was financially supported by the Natural Science Foundation of China (No. 21672082) and Shandong Key Development Project (No. 2016GSF201209).

Compliance with ethical standards

Conflict of interest The authors declare that they have no conflict of interest.

References

- Barreiro EJ, Camara CA, Verli H, Brazil-Más L, Castro NG, Cintra WM, Aracava Y, Rodrigues CR, Fraga CA (2003) Design, synthesis, and pharmacological profile of novel fused pyrazolo [4,3-*d*]pyridine and pyrazolo[3,4-*b*][1,8]naphthyridine isosteres: a new class of potent and selective acetylcholinesterase inhibitors. *J Med Chem* 46:1144–1152
- Bartus RT, Dean RL, Beer B, Lippa AS (1982) The cholinergic hypothesis of geriatric memory dysfunction. *Science* 217:408–414
- Bhat MA, Al-Omar MA, Siddiqui N (2013) Antimicrobial activity of Schiff bases of coumarin-incorporated 1,3,4-oxadiazole derivatives: an in vitro evaluation. *Med Chem Res* 22:4455–4458
- Cheung J, Rudolph MJ, Burshteyn F, Cassidy MS, Gary EN, Love J, Franklin MC, Height JJ (2012) Structures of human acetylcholinesterase in complex with pharmacologically important ligands. *J Med Chem* 55:10282–10286
- Dandriyal J, Singla R, Kumar M, Jaitak V, (2016) Recent developments of C-4 substituted coumarin derivatives as anticancer agents *Eur J Med Chem* 119:141–168
- Delogu GL, Matos MJ, Fanti M, Era B, Medda R, Pieroni E, Fais A, Kumar A, Pintus F (2016) 2-Phenylbenzofuran derivatives as butyrylcholinesterase inhibitors: synthesis, biological activity and molecular modeling. *Bioorg Med Chem Lett* 26:2308–2313
- Demir Özkay Ü, Can ÖD, Sağlık BN, Turan N (2017) A benzothiazole/piperazine derivative with acetylcholinesterase inhibitory activity: Improvement in streptozotocin-induced cognitive deficits in rats *Pharmacol Rep* 69:1349–1356
- Ellman GL, Courtney KD, Andres V, Feather-Stone RM (1961) A new and rapid colorimetric determination of acetylcholinesterase activity. *Biochem Pharmacol* 7:88–95
- Feng B, Li X, Xia J, Wu S (2017) Discovery of novel isoflavone derivatives as AChE/BuChE dual-targeted inhibitors: synthesis, biological evaluation and molecular modelling. *J Enzy Inhib Med Chem* 32:968–977
- Furuya T, Kamlet AS, Ritter T (2011) Catalysis for fluorination and trifluoromethylation. *Nature* 473:470–477
- Girisha HR, Narendra Sharath Chandra JN, Boppana S, Malviya M, Sadashiva CT, Rangappa KS (2009) Active site directed docking studies: synthesis and pharmacological evaluation of cis-2,6-dimethyl piperidine sulfonamides as inhibitors of acetylcholinesterase. *Eur J Med Chem* 44:4057–4062
- Hassan MZ, Osman H, Ali MA, Ahsan MJ (2016) Therapeutic potential of coumarins as antiviral agents. *Eur J Med Chem* 123:236–255
- Herrmann N, Chau SA, Kircanski I, Lanctot KL (2011) Current and emerging drug treatment options for Alzheimer's: disease a systematic review. *Drugs* 71:2031–2065
- Hoerr R, Noeldner M (2002) Ensaculin (KA-672 HCl): a multi-transmitter approach to dementia treatment. *CNS Drug Rev* 8:143–158
- Huey R, Morris GM, Olson AJ, Goodsell DS, (2007) A semiempirical free energy force field with charge-based desolvation *J Comput Chem* 28:1145–1152
- Inoue T, Wang F, Moriguchi A, Shirakawa K, Matsuoka N, Goto T (2001) FK960, a novel potential anti-dementia drug, enhances high K⁺-evoked release of somatostatin from rat hippocampal slices. *Brain Res* 892:111–117
- Jameel E, Umar T, Kumar J, Hoda N (2016) Coumarin: a privileged scaffold for the design and development of antineurodegenerative agents. *Chem Biol Drug Des* 87:21–38
- Li H, Yao Y, Li L (2017) Coumarins as potential antidiabetic agents. *J Pharm Pharmacol* 69:1253–1264
- Li JC, Zhang J, Rodrigues MC, Ding DJ, Longo JP, Azevedo RB, Muehlmann LA, Jiang CS, (2016) Synthesis and evaluation of novel 1,2,3-triazole-based acetylcholinesterase inhibitors with neuroprotective activity *Bioorg Med Chem Lett* 26:3881–3885
- Matsuoka N, Aigner TG (1997) FK960 [*N*-(4-acetyl-1-piperazinyl)-*p*-fluorobenzamide monohydrate], a novel potential antidementia drug, improves visual recognition memory in rhesus monkeys: comparison with physostigmine. *J Pharmacol Exp Ther* 280:1201–1209
- Morris GM, Goodsell DS, Halliday RS, Huey R, Hart WE, Belew RK, Olson AJ (1998) Automated docking using a Lamarckian genetic algorithm and an empirical binding free energy function. *J Comput Chem* 19:1639–1662
- Mosmann T (1983) Rapid colorimetric assay for cellular growth and survival: application to proliferation and cytotoxicity assays. *J Immunol Methods* 65:55–63
- Nachon F, Carletti E, Ronco C, Trovaslet M, Nicolet Y, Jean L, Renard P (2013) Crystal structures of human cholinesterases in complex with huprine W and tacrine: elements of specificity for anti-Alzheimer's drugs targeting acetyl and butyrylcholinesterase. *Biochem J* 453:393–399
- Revankar HM, Bukhari SN, Kumar GB, Qin HL (2017) Coumarins scaffolds as COX inhibitors. *Bioorg Chem* 71:146–159
- Talesa TN (2001) Acetylcholinesterase in Alzheimer's disease. *Mech Ageing Dev* 122:1961–1969
- van Greunen DG, Cordier W, Nell M, van der Westhuyzen C, Steenkamp V, Panayides JL, Riley DL (2017) Targeting Alzheimer's disease by investigating previously unexplored chemical

- space surrounding the cholinesterase inhibitor donepezil. *Eur J Med Chem* 127:671–690
- Weinstock M (2012) Selectivity of cholinesterase inhibition. *CNS Drugs* 12:307–323
- Więckowska A, Więckowski K, Bajda M, Brus B, Sałat K, Czerwińska P, Gobec S, Filipek B, Malawska B (2015) Synthesis of new N-benzylpiperidine derivatives as cholinesterase inhibitors with β -amyloid anti-aggregation properties and beneficial effects on memory in vivo. *Bioorg Med Chem* 23:2445–2457
- Yu YF, Huang YD, Zhang C, Wu XN, Zhou Q, Wu D, Wu Y, Luo HB (2017) Discovery of novel pyrazolopyrimidinone derivatives as phosphodiesterase 9A inhibitors capable of inhibiting butyrylcholinesterase for treatment of Alzheimer's disease. *ACS Chem Neurosci* 8:2522–2534